Available online at www.sciencedirect.com

ScienceDirect

Coordination Chemistry Reviews 252 (2008) 155–169

COORDINATION CHEMISTRY REVIEWS

www.elsevier.com/locate/ccr

Review

Platinum OMCVD processes and precursor chemistry

Cyril Thurier, Pascal Doppelt*

Institut de Chimie et des Matériaux Paris-Est (UMR 7182), 15 rue Georges Urbain, 94407 Vitry-sur-Seine, France

Received 22 January 2007; accepted 4 April 2007
Available online 8 April 2007

Contents

---

* Corresponding author. Tel.: +33 1 56 70 30 19; fax: +33 1 46 75 04 33.
E-mail address: pascal.doppelt@cecm.cnrs.fr (P. Doppelt).

doi:10.1016/j.ccr.2007.04.005

Abstract

Chemical Vapor Deposition (CVD) is an advanced manufacturing technology for surface coating currently enjoying intense development. Particularly, platinum Organometallic Chemical Vapor Deposition (OMCVD) is a technique allowing the formation of platinum thin films as a fine dispersion of platinum particles. This article reviews the current knowledge of platinum OMCVD and relates all the factors investigated in its recent development. Appreciable progress has been made during the two last decades due to varied experimentations with precursors and operating conditions. The different techniques (e.g. LCVD, PECVD, IACVD, EBCVD, FBCVD) used for platinum OMCVD are described with extended discussions about their own advantages and drawbacks, each technique being consistent with particular applications. The influence of gases, solvents and substrates will be discussed through many examples leading to the comprehension of growth and nucleation mechanisms in the platinum deposits. Attention is focused particularly on the behaviour in CVD of the various organometallic precursors and their own performances. The results obtained are detailed in terms of conditions, growth rate, purity and resistivity in order to give a full scope to this domain.

Keywords: Platinum precursors; Platinum thin films; OMCVD processes

1. Introduction

Even though the first example of platinum CVD (Chemical Vapor Deposition) was reported in 1947, it was not until the late 1980s that significant development took place. The major applications found in the literature are the preparation of electrodes for microelectronics, ohmic and schottky diode contacts, diffusion barriers, coatings for high temperature crucibles and the preparation of solid supported catalysts. Platinum has very good electrical conductivity and many catalytic properties. It should be noted that in some cases, the deposit is obliged to be presented as a continuous film whereas in other cases, catalysts for example, they are preferred in the form of a dispersion of particles with a high surface area. The principle of an OMCVD process is to vaporize a metal-containing precursor, usually an organometallic complex which undergoes thermal decomposition, followed by deposition onto the substrate to form a metal layer. In practice, vaporization is performed under pressure and temperature conditions that allow a precursor vapor pressure sufficient for film deposition to be obtained, while maintaining the integrity of the precursor complex. The substrate is heated beyond this stability range, causing the decomposition of the organometallic species and the formation of metallic particles. CVD has various advantages compared to other deposition techniques for example; pyrolysis temperature in OMCVD is hundreds of degrees lower than for other techniques. Moreover the method has a high throwing power in cavities and the films obtained are often dense and continuous, avoiding porosity incompatible with good electrical properties. Contrary to the liquid impregnation method, CVD is fast and the stages of impregnation, washing, drying, calcination and activation are avoided. Also avoided are surface poisoning and the material transformations activated during drying. It is thus a fast and economic method to obtain controlled deposits of high quality. The main drawbacks of OMCVD are the possible incorporation of impurities due to non-exhausted remains and poor adhesion of the film in some cases. Although papers reviewing platinum OMCVD have been already published [1–3], we present here an exhaustive review based on precursor chemistry. It is notable that most of the papers dealing with platinum MOCVD since 2005 concerns the technologic side or particular applications (e.g. fuel cell, alloys) demonstrating there the maturity of the art.

2. Deposition techniques based on CVD applied to platinum deposition

The “traditional method” for OMCVD consists of vaporization of the precursor at low temperature, under reduced pressure and to deposit a metal film, for example, on a substrate surface at higher temperature by adsorption and thermal decomposition of the precursor. The various parameters that control this deposition technique will be further described. Alternative methods will also be described where the necessary energy for precursor decomposition is brought by another energy source.

The various stages of the process are (Fig. 1):

(1) convection of the gaseous reagents
(2) diffusion of the reagents towards the substrate
(3) adsorption of the reagents onto the substrate

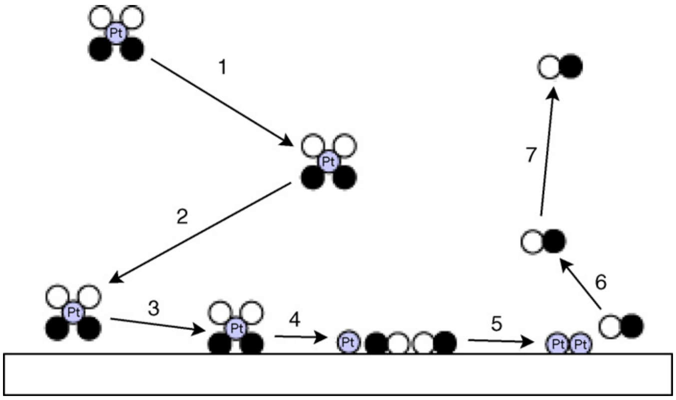

Fig. 1. Stages of a “traditional” MOCVD process.

(4) chemical reaction of the adsorbed species producing nuclei and further reaction to give a metal film
(5) desorption of the gas products of the reaction
(6) diffusion of these products through the boundary layer
(7) gas evacuation of the system.

The reader must keep in mind that for all deposition techniques described in this chapter, factors determining if the system is surface-limited or transport-limited (consumption or not of all incoming precursor to the diffusion layer) remain the same: temperature, flow rate, pressure, reactor and substrate geometry. All these parameters are discussed elsewhere [4]. Diffusions at the boundary layer are a complex phenomenon and results cannot be applied directly from a system to another.

The choice of a CVD method among all those described will be made regarding specifications of the deposit in terms of topology, purity, physical properties, process speed and cost.

2.1. Laser induced chemical vapor deposition (LCVD)

In this case, the decomposition is induced with a laser beam. LCVD has the advantages of better control of the decomposition mechanism compared to the traditional method and being able to function on a substrate-limited surface. This method allows the deposition in confined zones and at low substrate temperature; e.g. from 30 to 100 °C with Pt(hfa)$_2$ **2** [5] (see the chemical structure). The process can be carried out with substrates that do not have high thermal conductivity and the deposit growth kinetics are often faster than those observed with traditional OMCVD. It is also possible to work at higher precursor pressure than in traditional CVD, growth kinetics being here limited by gas-phase decomposition. Nevertheless, for most of the applications considered currently: repair of circuits, manufacture of prototypes, etc., the writing speed remain slow (several μm s^{-1}, depending on conditions). Deposit resistivity can be optimized toward deposition rate and laser power. Optimums require deposition rate neither too slow nor too fast and laser power neither too weak nor too strong. Partial pressure of precursor seems to be the critical factor, allowing an increase in the deposition rate without loss in the overall deposit quality [6]. To obtain a film with few impurities, the laser must de-coordinate all the precursor ligands; avoiding the incorporation of carbon and other elements into the film. The growth rate depends on the wavelength of light used and on the laser power. Photolysis can occur in several stages with quantum yields also dependent on the laser wavelength. Another phenomenon can occur when overheating of the deposit by the laser leads to the precursor desorption [5]. When the laser induces excess heating of the substrate, the deposition cannot be considered as pure LCVD, the precursor decomposition becoming primarily thermal and no longer photolytic (Fig. 2).

This method has been used with the precursor Pt(hfa)$_2$ **2** with an argon laser (458 and 514 nm) [7]. Increased precursor partial pressure led to the formation of a thicker deposit and by increasing the power of the laser, the consequent increase of the deposition temperature led to side growth. The more regular film morphologies are observed at relatively low power and low writing speed. The thermochemical growth of platinum thus depends on the thermal properties of the substrate [8]. Other studies have showed that the side growth occurs when the mode is controlled by the kinetics [9]. Axial growth occurs when the mode is controlled by the diffusion of the reagents. In order to be in a kinetically controlled regime, it is necessary to have a laser spot of a rather large diameter: e.g. ≥15 μm [7].

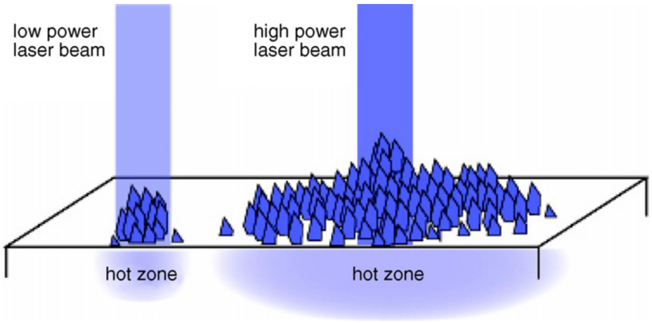

Fig. 2. Lateral growth induced by heating effect of the laser. Using a too high laser power increases the substrate temperature and permits the thermal decomposition of the precursor.

LCVD studies were also carried out with CpPtMe$_3$ **6** under the following conditions: the precursor was heated to 56 °C (affording a partial pressure of 0.33 Torr) and transported by argon (120 mL/min) to the cell. Hydrogen introduction was proceeded close to the substrate: glass, silica, sapphire, silicon or GaAs at room temperature [10]. A XeCl laser (308 nm) was used producing a spot of 1 mm radius with pulses of 2.6 mJ at 10 Hz. In 10 min, a deposit 100 nm thick was obtained. The observations above, affirm that the mechanism in this case, without hydrogen, is different from the thermal mechanism (Fig. 3): there is real photochemical reaction that takes place (homolysis of the Pt–CH$_3$ bond) then adsorption on the surface of the formed complex and thermal reaction leading to the decoordination of the Cp ligand. In the presence of hydrogen, the mechanism proposed for the photolysis proceeds by an oxidative addition of dihydrogen followed by of reductive elimination of methane.

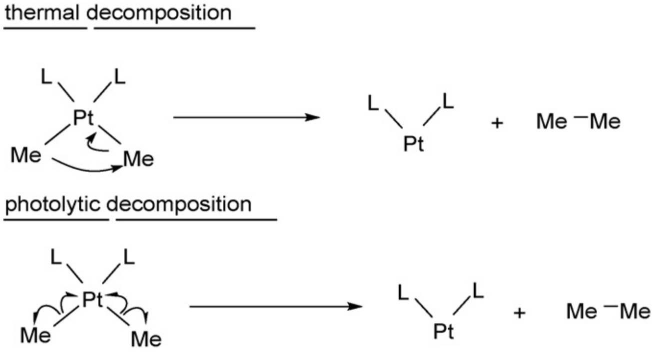

Fig. 3. Postulated thermal and photolytic mechanisms of dialkyl(II) platinum precursor decomposition during CVD.

2.2. UV induced chemical vapor deposition.

The OMCVD can also be carried out under the irradiation of a UV lamp, which can improve the process of nucleation of platinum while lowering the operational deposition temperature. In the case of platinum deposition, two methods are described [11,12], the first, consisting of depositing the precursor on the substrate then irradiation; the second, being deposition of platinum directly by adsorption, followed by decomposition of the precursor by irradiation of the substrate. The solid precursors $CpPtMe_3$ **6** and liquid $MeCpPtMe_3$ **7**, evaporated by an argon bubbling (1000 sccm = 1000 standard cubic centimetres per minute) at a pressure from 1 to 10 Torr at 25 °C, lead to a deposited film thickness from 5 to 40 nm in 30 s with the assistance of a UV lamp (260 nm). Without a lamp, decomposition of such precursors is insignificant at room temperature and remains slow at higher temperature in absence of reactive gases. Typically, $MeCpPtMe_3$, **7** leads to a deposited film 6 nm thick in 30 s at 120 °C on silicon.

2.3. Plasma enhanced platinum CVD (PECVD)

Plasma generated by radiofrequency has been used to enhance platinum CVD. $CpPtMe_3$, **6** was used to obtain Pt thin films by PECVD in the presence of oxygen at temperatures as low as ambient temperature [13]. The films obtained are nearly 100% pure although their resistivity is high, 46 $\mu\Omega$ cm, which is four times that of bulk platinum (10.8 $\mu\Omega$ cm). The film purity depends on the deposition temperature, on the plasma power, and also on the equipment used. The precursor $MeCpPtMe_3$, **7** was deposited on silicon carbide nanowires by PECVD [14] under the following conditions: **7** is heated to 70 °C and introduced into the reactor by an argon flow (2.5 sccm) at a total pressure of 600 mTorr. The deposit is carried out on the substrate at 300 °C using an RF plasma (13.56 MHz). Argon is used at the same time as carrier gas for generating the plasma. In 12–15 min, a particulate deposit of 2.76 ± 0.46 nm; corresponding to 31,000 particles per μm^2 was observed. The film is very dense, homogeneous, continuous and adherent. Increasing the temperature led to larger particle size. PECVD processes can also lead to very heterogeneous material deposit when two different precursors are mixed. For example, the mixture of $Pt(acac)_2$, **1** and tetramethyl tin generates, under plasma, in the presence of oxygen a layer of SnO_2 containing dendritic platinum fractal structures [15]. $Pt(acac)_2$, **1** has also been deposited by micro-capillary plasma. Resulting film thickness can reach more than 100 nm in a Pyrex chip [16].

2.4. Focused ion-assisted Chemical Vapor Deposition (IACVD) of platinum films and 3D structures

Ion beams have been used for the local deposition of platinum OMCVD [17] in which resistivity is 10–5000 times higher than that of pure platinum [18,19], due to the incorporation of elemental impurities, such as C (from the precursor), O (from the residual gas) and Ga resulting from the Ga^+ beam employed for the deposition process. In ion-assisted deposition, the ion beam decomposes an adsorbed layer of an organometallic precursor. This decomposition generates metal atoms on the surface of the substrate; the organic fragments diffuse away and are exhausted from the system. Film composition will therefore depend on the efficiency of precursor dissociation as well as the efficiency of volatile by-product diffusion away from the sample surface. These two parameters both should depend on the relative arrival rates of Ga^+ ions and of precursor molecules on the sample surface. The effects of Ga^+ ion and precursor fluxes on the deposited films composition and resistivity have been determined. Results show that increasing precursor flux at constant ion flux increases Pt and C, but decreases Ga content of the film. Increasing ion flux, at constant precursor flux, increases Pt content, while decreasing C content of the film. Resistivity did not depend on the film thickness nor on temperature [18], but was shown to follow C content; films with lower C content having lower resistivity.

The use of $MeCpPtMe_3$, **7** with a beam of Ga^+ at 30 keV and 1000–6000 pA led to 50–200 nm thick films on squares of (1 0 0) boron-doped silicon substrates.

Deposition in trenches and at near grazing incidence was found to occur with a high yield. Lines up to 0.2 μm high and 0.3 μm wide have been thus deposited at near grazing incidence. The highest platinum content in the film is 46% (Ga 28%, C 24%, O 2%) with an ion beam current of 78 pA. The growth of discrete platinum islands instead of a plain line may be due to a shadowing effect depending on the beam incidence.

2.5. Electron Beam Chemical Vapor Deposition (EBCVD)

Electron Beam Chemical Vapor Deposition (EBCVD) is a technology that uses an electron beam to provide localized deposition for nanoscale structures or device fabrication.

In EBCVD, primary electrons from the beam impact a substrate, causing secondary electrons to be emitted. These secondary electrons play a prominent role in dissociating adsorbed reagent molecules to form a deposit on the substrate and volatiles that are then evacuated from the chamber. The deposition process depends on many factors including the precursor and the electron beam properties. If the electron beam is not moved relative to the substrate, a dot is grown. A fibre is grown if the growth time is increased. If the beam is moved, lines or other structures can be deposited as in rapid prototyping. High aspect ratio structures can be deposited as supertips on atomic force microscope tips to improve resolution. The resolution of the structures obtained (20 nm for a beam of 30 kV and 7 nm for 200 kV) are better than those obtained with LCVD (10–100 μm, see above) or with ions beams (100 nm). Electric interconnection lines can be elaborated by 25–30 nm point juxtaposition [20]. Using $CpPtMe_3$ **6**, Takai et al. [21] reported fibre growth from 0.06 to 0.6 μm^3/min and spots of 3 nm with 30 keV and 70–100 pA at 10^{-6} Torr. The best growth rates obtained reached 9 μm/min [22]. Studies with $MeCpPtMe_3$, **7** showed that increasing the voltage permitted to thinner fibres and increasing the beam current raised the vertical growth rate [23]. Although deposits resulting from the application of EBCVD contain a lot of carbon [24], the EBCVD method offers advantages over IACVD: leaving fewer impurities in the deposit and degrading the substrate less [25]. A post-treatment consisting of a heating step in the presence of oxygen decreases the level of impurities. The deposit may then suffer from a volume reduction due to carbon impurity elimination.

Electron beam induced deposition of Pt thin films on a Cr-coated Si(1 0 0) substrate has also been investigated with $[Pt(PF_3)_4]$, **5** [26]. According to Auger electron spectroscopy, the Pt content reached 60 atomic % for a 3 kV e-beam flux of 2.1×10^{-2} A cm^{-2}, a precursor pressure of 2×10^{-5} Torr, and a substrate temperature of 80 °C. As the flux ratio (e-beam to precursor) increased above the optimized value of 10, the rate shifted from control by the e-beam flux to the precursor flux. The phosphorus content was reduced by adding O_2.

2.6. Fluidized Bed Chemical Vapor Deposition (FBCVD)

Fluidized Bed Chemical Vapor Deposition (FBCVD) is one of the most efficient techniques to functionalize, to deposit on, or to coat each individual particle of a powder from gaseous species. FBCVD combines two processes. One is the deposition itself, the other aims in suspending the particles in the deposition zone, most often by flowing a gas upwards through the powder and in bringing heat to the powder [27]. In contrast to CVD on flat surfaces which often operates in a surface kinetics limited regime, FBCVD is generally transport-limited.

This is due to the extremely high available growth surface to heated volume ratios (S/V) in the deposition area. Consequently, gaseous precursors are very often totally consumed a few centimetres after their entrance into the fluidized bed reactor, but the high degree of gas solid mixing compensates for this discrepancy, and ensures isothermal conditions and uniform deposition.

2.7. Atomic Layer Deposition (ALD)

Layer-by-layer deposition processes have been tested with platinum precursors. Precursors, air or oxygen and inert gases are introduced to the reactor in alternate pulses onto the hot substrate. A single atomic layer is formed through an auto-limited growth mechanism. The complex partially decomposes by consuming all the available oxygen adsorbed on the platinum surface and the following oxygen pulse will finish the decomposition. Decomposition products are CO_2, water and hydrocarbon residues if present in the starting precursor. Film growth using $MeCpPtMe_3$, **7** as a precursor is limited by the precursor saturation, then short time pulses are needed to obtain a fast deposition—duration of the pulses are, respectively, $\leq$0.5 s for precursor and $\leq$1.5 s for the air. Out of these short durations, the observed deposition mode is not pure ALD and deposition rate is lower, the deposits formed during a cycle being too thick to allow a full action of oxygen. Oxygen adsorbs only on superficial platinum and subsequent oxide layer is insufficient to react with the total amount of precursor in the next cycle. Film growth is slow when the deposition starts because of the nucleation step. The films obtained are much uniformed and have a rough surface and highly oriented grains. Adhesion of the films on these substrates was modest but the amount of all impurities is low and decreases as the air pulse time increases. When the air pulse time was increased from 1.0 to 2.0 s, the maximum hydrogen content decreased from 1.0 to 0.5 at.%, the maximum carbon content decreased from 1.0 to 0.5 at.% and the maximum oxygen content decreased from 2.0 to 1.0 at.%. The resistivity of the platinum film was low (down to 12 μΩ cm), close to that of bulk platinum (10.8 μΩ cm) [28,29]. $Pt(acac)_2$, **1** has been shown to be a less desirable precursor than $MeCpPtMe_3$, **7** for ALD deposition [30]. Indeed, this precursor decomposes on the walls of the source furnace under the ALD conditions: 0.6–1 mBar at 155 °C. This decomposition limits its application and makes it also unsuitable for the use in ALD conditions.

3. Solvents used for liquid delivery systems

In the first examples of platinum OMCVD, the solid precursors were heated under reduced pressure for vaporization. These solids can vary in their shape or crystallinity which can affect their volatility. Various systems of vaporization have been developed and adapted for use with pure liquid precursors or solutions [31]. The first system described is that of the bubbler, where the precursor is pulled through the liquid by the bubbling of a gas. The liquid can be heated (and the entire line, up to the reaction chamber to avoid re-condensation) or cooled according to the volatility of the precursor and the desired precursor flow. This system was adapted with regulators and sensors in order to have a partial pressure of precursor constant in the furnace. A direct liquid injection system has been described where the solution is injected by syringe directly into a vaporization chamber. The syringe can be replaced by volumetric pumps; mixing the solvent and precursor and delivering the solution in a constant fashion or according to a pre-programmed set of instructions. An improvement to systems in terms of precision was the development of pulsated liquid injection where micro-quantities of precursor solution are injected sequentially.

A comparative OMCVD Pt film study under very similar experimental conditions, employing two precursor delivery systems, has been reported: comparing Pt OMCVD films obtained from $MeCpPtMe_3$, **7** with a TriJet^{TM} liquid delivery system and a conventional bubbler [32]. The properties of the deposits grown using the two different precursor delivery systems were found to be very similar, making a comparison between the two deposition techniques non-trivial. In this study, the use of cyclohexane gave positive results due to its low chemical interference with the oxidative decomposition of platinum precursor. Although the use of a conventional bubbler leads to fast deposition of Pt films, controlling of amount of consumed precursor is difficult. Conversely, the liquid injection system enables perfect control over the quantity of precursor used, but results in a slower rate of film growth. In the framework of OMCVD Pt deposits used as bottom electrodes in ferroelectric capacitors, the possibility to control the precursor consumption is a key issue due to the expense of the platinum precursor. Hence, the major motivation for the utilization of direct liquid injection of the precursor would be to control the metallization process costs. Even for liquid precursors, the use of a solvent is often needed to control precursor delivery. Aerosol flash evaporation using solutions give good results in terms of accuracy.

In general, the choice of solvent remains unexplained and its effects upon deposition are not described in detail. They can play a role by interacting with the second even the first sphere of metal coordination and thus stabilize the metal complex. It is also possible to dissolve in the solution a suitable quantity of free ligand in order to stabilize the complex. Hence, 1,4-pentadiene was described as being able to inhibit the decomposition of the precursor *cis*-bis(η^2,η^1-pent-4-en-1-yl)Pt **11** in solution [33]. The free ligand can also inhibit the formation of the deposit while being adsorbed on the film [34]. Another potential effect of solvent is to increase the vapor pressure of the precursor by an azeotropic effect.

The more commonly used solvents are: the acetylacetone with Pt(acac)$_2$ **1** [35], pentane for (cod)Pt(Me)$_2$ **14** [36] and cyclohexane for MeCpPtMe$_3$ **7** [37]. Other examples are described including THF for MeCpPtMe$_3$ **7** [38,39] or Pt(acac)$_2$ **1** [38] and *n*-hexane for EtCpPtMe$_3$ [40].

4. Platinum precursors

Contrary to metals as nickel, where the complexes Ni(CO)$_4$ carbonyls were very early used because of their excellent volatility, the carbonyl complex Pt(CO)$_4$ is not thermally stable. Carbonyls complexes of platinum can however be stabilized by the presence of another ligand such as phosphine. Many complexes have been developed, and among alls, a β-diketonate family, a trimethyl-cyclopentadienyl family and (cod)Pt(Me)$_2$ involve the most met precursors in the literature. OMCVD precursors' specifications enclose a good volatility, an adequate stability window, a low production cost, few elemental impurities in the film, fast nucleation and low risk handling: stability toward moisture and oxygen (no pyrophoricity!) and low toxicity.

4.1. The β-diketonate family complexes

*4.1.1. Pt(acac)$_2$ **1***

The first tests were carried out with square planar complex Pt(acac)$_2$, **1** by Marboe [41]. The vaporization from Pt(acac)$_2$ **1** to 180 °C (20–200 μTorr) followed by deposition on a hot glass (350–450 °C) led to the formation of an adhesive mirror like film. Subsequently, Rand showed that under these conditions, the obtained film is rich in carbon and that in the presence of hydrogen, the deposit is much purer, however, the precursor is partially decomposed before vaporization [42]. Kwak showed indeed that **1** is stable only until approximately 160 °C [43]. By vaporizing the complex at 140 °C and by depositing it in the presence of oxygen at 450 °C, he obtained films with few carbon impurities and a high degree of crystallinity. Beyond a deposition temperature of 450 °C, the obtained films in the presence of oxygen present grains randomly oriented, whereas at 280 °C, three distinct structures are observed within the one film: cauliflower structures, structures in columns and equiaxial grains with large specific surfaces [44]. This precursor can decompose from 155 °C on the furnace walls what limits its application in ALD [30]. With Pt(acac)$_2$ **1**, substrate temperature have to be chosen quite far away from its stability range because only partial decomposition occurs at 155 °C and a temperature of 280 °C is required to obtain a metallic film. This is the case because Pt(acac)$_2$ **1** decomposes in several stages at different temperatures.

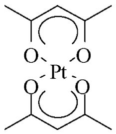

Pt(acac)$_2$

1

Pt(acac)$_2$, **1** however has the advantage of being not very expensive and not very sensitive to water and air. Goswani showed that the decomposition kinetics controls the crystallites growth by allowing precursor adsorption and surface diffusion, nucleation rate is also affected (vide infra) [38]. Paradoxically, Pt–O bonds are very stable, more stable than Pd–O [45] and comparable to C–C bonds (Pt–O$_{\text{acac}}$: 180 kJ mol^{-1} [46], mean values for C=C: 250 kJ mol^{-1}, C–C: 140 kJ mol^{-1}). It is thus the ligand which decomposes without metal de-coordination, films with high levels of impurities are generally formed. This precursor was described like being able to initialize the deposit of other precursors to make mixed deposits. It allows the deposition of Si(OEt)$_4$ at 320 °C instead of 600 °C leading to a Pt/SiO$_2$ mixture [47].

The following complexes are derived from Pt(acac)$_2$.

*4.1.2. Pt(hfa)$_2$ **2***

After the first satisfactory CVD tests of Pt(acac)$_2$ **1**, a fluorinated version of this complex was synthesized in order to increase the difference between the precursor vaporization and the decomposition temperatures. Pt(hfa)$_2$ **2** was tested first by LCVD [5,7] (Laser Chemical Vapor Deposition) then in conventional thermal CVD. As for Pt(acac)$_2$ **1**, the oxygen addition during deposition limits the amount of carbon impurities obtained in Pt films on SiO$_2$/Si substrates [48]. Compound **2** is very stable and it can be present in the film at temperatures as high as 400 °C staying not decomposed. The deposited films usually contain fluorine, significant amounts of carbon and oxygen. Although less volatile, Pt(acac)$_2$ **1** can be preferred to Pt(hfa)$_2$, **2** because removal of the fluorine impurities can be difficult to process [47]. Contrary to other impurities, the fluorine cannot be eliminated easily later, this one being persistent even after an argon plasma abrasion. Fluidized bed CVD studies have shown that the addition of hydrogen allows the deposition temperature to be lowered from 400 to 140 °C giving 10–100 nm diameter grains in the shape of pyramid however, the obtained film adhesion is poor [49]. Carbon and oxygen impurities are also present and the deposited film is not homogeneous. Stepwise adsorption is apparent, the silica taking the colour of the precursor successively, followed by that of metal. The decomposition is incomplete and slow even at high temperatures. Long duration and high partial pressures of hydrogen and the ligands de-coordinate to lead to non-volatile species.

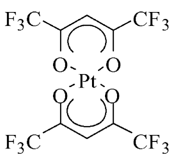

Pt(hfa)$_2$

2

Fluorine-free complexes derived from Pt(acac)$_2$, **1**, **3a** and **3b**, bearing dissymmetric ligands is also efficient as platinum precursors [50]. The dissymmetry of the ligands here may help to enhance volatility.

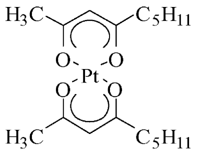

3a

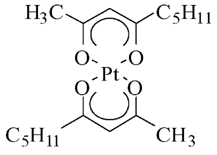

3b

4.2. Precursors with carbonyl and phosphine ligands

4.2.1. cis-Pt(CO)$_2$Cl$_2$, 4

Complex **4** has been tested as a precursor for CVD on various substrates [51]. The temperature of the saturator was approximately 100–150 °C, while CO was used as a carrier gas to prevent precursor decomposition. Indeed, in absence of CO, the residual not sublimated solid contains involatile PtCl$_2$ revealing precursor decomposition. The CVD film deposited was irregular with a poor adherence. Moreover, the use of CO is problematic, since it reacts with iron and nickel of the equipment to give volatile metallic species, thus producing a source of contamination. This method also generates toxic vapors (phosgene). In the presence of hydrogen, the deposit was of better quality but displayed a poor adherence on the substrate—in this case silicon. PtMe(η^1-C$_5$H$_5$)(CO) has been synthesized by Xue as an alternative carbonyl-containing precursor, and used for CVD. However, being unstable it was difficult to store [52].

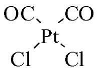

4

4.2.2. Pt(PF$_3$)$_4$, 5

This precursor is a stable Pt(0) complex described in 1969 [53] and with a tetrahedral structure [54]. Its decomposition occurs *via* the de-coordination of all phosphine ligands and does not involve a reductive step. Pt(PF$_3$)$_4$, **5** has been used as precursor for CVD experiments since 1973 [42,51]. It has excellent volatility, being liquid at ambient temperature and atmospheric pressure with a boiling point of 87 °C. PF$_3$ is similar to CO in reactivity with respect to metals. This compound can nevertheless attack SiO$_2$, which can complicate the pyrolysis process. When mixed with hydrogen, at a pressure partial of 15 Torr, deposition at 200–300 °C leads to a continuous film with good adhesion on Al$_2$O$_3$, but containing P and F impurities, which modified the mechanical and electronic properties of the film obtained. The process of phosphorus diffusion was also studied as a way to dope silicon [55] however, the silicon based materials obtained do not have properties sufficiently interesting for applications in microelectronics.

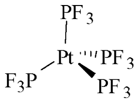

5

4.3. Trimethyl-cyclopentadienyl platinum precursors

4.3.1. CpPtMe$_3$, 6

This precursor is a platinum(IV) complex and its decomposition also occurs *via* the reductive de-coordination of all ligands.

CpPtMe$_3$, **6** and its derivatives (Table 1), are the most abundantly described precursors for CVD. First described in CVD in 1988 as an interesting alternative to the other precursors, it can be used under milder conditions compared with those necessary for the preceding precursors and gives higher quality films [56]. Moreover, CpPtMe$_3$, **6** is quite volatile with a partial pressure of precursor of 0.05 Torr at 25 °C. The deposition at 180 °C on glass or silicon in the presence of hydrogen led to films formed by 100 nm cubic crystallites with a growth rate of 0.1 Å s^{-1}. The platinum films contain oxygen on the surface and carbon traces throughout (<1%) [57]. This precursor can decompose so rapidly in the presence of hydrogen on initially deposited film, under CVD conditions, that the deposition growth rate is limited by the supply of the organometallic species (see also Section 8) [52].

Table 1
Physical properties of (cyclopentadienyl)trimethylplatinum precursors used for platinum OMCVD

Precursors	Some physical characteristics [46,48,49]
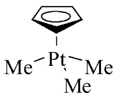	$\mathrm{Ln}(P_{\mathrm{vap}}(\mathrm{Torr})) = (25.9 - 8.59) \times 10^3/(T\,(\mathrm{K}))$; $P_{\mathrm{vap}} = 0.044$ Torr at 23 °C; m.p. = 108.5 °C
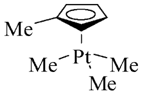	$\mathrm{Ln}(P_{\mathrm{vap}}(\mathrm{Torr})) = (26.1 - 8.69) \times 10^3/(T\,(\mathrm{K}))$; $P_{\mathrm{vap}} = 0.053$ Torr at 23 °C; m.p. = 30 °C
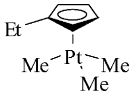	$P_{\mathrm{vap}} = 0.1$ Torr at 39 °C, 1 Torr at 71 °C; m.p. < −78 °C

The synthesis of **6** described by Kaesz utilizing $Pt(Me)_3I$ and $Na(C_5H_5)$ provides a yield of 52% [56]. A method with a yield of 89% was described by Gilman [58]. The principal disadvantage of this precursor is its sensitivity to air (oxygen and water).

4.3.2. *MeCpPtMe$_3$, **7***

In order to increase the precursor volatility, one hydrogen of the cyclopentadienyl ligand was substituted by a methyl group. The precursor $MeCpPtMe_3$, **7** thus obtained, has a melting point of 30 °C. The main inconvenience with respect to handling of $MeCpPtMe_3$, **7** is its sensitivity toward oxygen and water similar to $CpPtMe_3$, **6**. A "one-pot" synthesis with a moderate yield (60%) starting from commercially available K_2PtCl_6 has been described, dibromoethane being preferable as a MeLi quencher instead of NH_4Cl [59].

When vaporized by argon bubbling (20 sccm) at 23 °C and mixed with hydrogen (20% by vol.), $MeCpPtMe_3$, **7** leads to a very clean deposit (<1 at.% C) as observed by XPS after surface sputtering (Fig. 4). Nevertheless, this reported impurity content has been discussed elsewhere and may be higher [60]. A high degree of poly-crystallinity was observed demonstrating a high nucleation rate and the formation of small crystallites. Observed growth rates are, respectively, 0.2 Å/s at 120 °C and 0.1 Å/s at 180 °C after an induction period [61]. Oxygen assisted deposition leads to an almost carbon free deposit [60,62]. Depositions have been realized by dissolving the precursor in hexane and then, by vaporizing the mixture at 50 °C by means of a TriJet^{TM} injector. A mixture of helium and oxygen was used as the carrier gas and deposit takes place on SiO_2/Si at 300–400 °C. Films with a thickness of 15–400 nm are formed that display a good resistivity (11 μΩ cm), homogeneous grain orientation, with a roughness of 2.4–5 nm and a grain size of 16–43 nm [32]. Because of its higher volatility, stability and its better ability to be completely decomposed at higher temperature, $MeCpPtMe_3$, **7** gives good results in ALD and the resulting films have a low resistivity [27,28]. It conveniently replaces $Pt(acac)_2$, **1**, which degrades at too low a temperature.

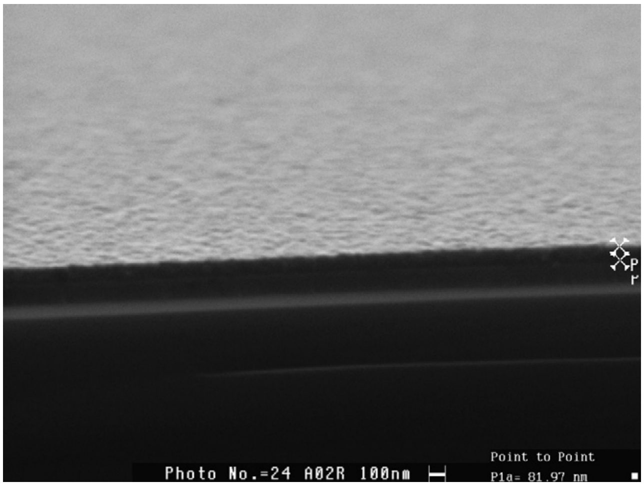

Fig. 4. SEM picture of a 45° view of the cross-section of a 82 nm thick Pt film obtained on a $TiO_2/SiO_2/Si$ by injection CVD from a cyclohexane solution of $MeCpPtMe_3$, **7**.

4.3.3. *EtCpPtMe$_3$, **8***

With the goal in mind of increasing the precursor volatility, a precursor containing an ethyl-cyclopentadienyl ligand was tested [40,63]. Deposits were carried out from 350 to 450 °C under 0.7–3 Torr, by vaporizing **8** dissolved in *n*-hexane at 130 °C (0.1 M). The carrier gas used was a mixture of Ar: 400 sccm and O_2, 100–1600 sccm, the substrate being silicon or SiO_2/Si heated to 280 or 340 °C. Contrary to the preceding complexes of the same family, $EtCpPtMe_3$, **8** is not oxygen and water sensitive. It is also able to form mixed Pt–C deposits [64]. A synthesis with a 51% yield of this precursor utilizing $Pt(Me)_3I$ and $Na(EtC_5H_4)$ was patented as well as the use of this precursor for Pt OMCVD [65]. The deposit is obtained by bubbling argon (20 sccm) in the pure precursor maintained at 35 °C at atmospheric pressure and heating of the substrate (Si) at 150 °C in the presence of hydrogen (50 sccm). A 40 nm film can thus be obtained in 20 min.

The use of the corresponding isopropylcyclopentadienyl and *tert*-butylcyclopentadienyl platinum complexes was also patented [59], and "one-pot" syntheses of these two complexes are patented, the one patent covering all three molecules.

4.4. *Olefin and allyl containing precursors (Fig. 5)*

4.4.1. *Pt(η^3-C_3H_5)$_2$ **9**, Pt(C_2H_4)$_3$ **10** and cis-bis(η^2,η^1-pent-4-en-1-yl)Pt **11***

Bis-allyl platinum compound **9** was tested in CVD. As in the case of $CpPtMe_3$, **6** its use results in rather pure deposits (1% carbon) [66] under relatively mild conditions (deposits at 250 °C and 10^{-4} Torr) [54]. Homoleptic allyl compounds are among the most volatile transition complexes for the third and second rows of the Periodic Table making them good candidates as precursors for CVD.

Compound **9** has been synthesized with a yield of 69% and can be sublimed at 25 °C at 10^{-4} Torr. However, **9** is not very stable and decomposes at temperatures as low as 20 °C. Other unstable but volatile compounds also result in very pure but amorphous films; for example, those obtained from $Pt(C_2H_4)_3$, **10** [61].

The precursor *cis*-bis(η^2, η^1-pent-4-en-1-yl)Pt **11** is also highly volatile and can be vaporized at room temperature. Pt films using **11** have been deposited on glass or copper at 200 °C [33]. The Auger analysis of the deposit on copper showed a constant composition on 125 nm of 65% platinum, 25% carbon,

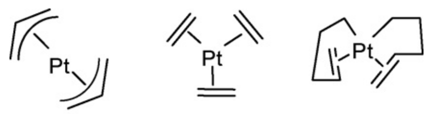

9 **10** **11**

Fig. 5. Chemical structure of poor stability olefin and allyl platinum precursors.

10% copper. This result can be improved at higher temperature (275 °C) at which smaller (60 nm diameter) and purer spherical platinum particles, with a composition of 82% platinum and 18% carbon, are formed.

4.4.2. *(cod)Pt(Me)$_2$, **14***

(cod)Pt(Me)$_2$ is a precursor which melts at 100 °C [67]. It was described by Kalck for its use in a fluidized bed CVD (FBCVD) for the heterogeneous preparation of catalysts and in CVD on graphite [36,49,68–72]. Platinum can thus be deposited by FBCVD on silica in 3 h at 120 °C at 40 Torr. The gas mixture contains helium, 3% hydrogen and 0.1% of the precursor **14**. Under these conditions, platinum particles can be obtained on which palladium particles can grow quickly. At 90 Torr with 1% hydrogen, the deposit on silica contains 2.3% by mass of 3 nm metal particles and a specific surface area of 175 m^2 g^{-1} [69]. When subjected to other conditions (30–60 Torr of helium containing 3–6% of hydrogen at 100–120 °C) **14** decomposes completely to form grains from 0.2 to 1 μm, containing 15% carbon when deposited on glass or 3 nm grains on silica in a fluidized bed.

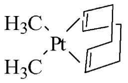

14

Deposition on highly ordered pyrolytic graphite (HOPG) can be performed by vaporization of a solution of **14** in pentane (10 mM) at temperatures of 60–180 °C. Deposition has also been carried out at 110 °C in the presence of 50 Torr of hydrogen on carbon fibres [70] or carbon nanospheres treated with nitric acid [71]. This latter treatment increases the concentration of nucleation sites and consequently a more homogeneous crystallite size deposit can be obtained. Finally, carbon nanospheres and carbon nanotubes were covered with platinum nanoparticles by fluidized bed CVD. Germination can only take place after a nitric acid treatment [72]. The particles obtained measure 2–3 nm on the carbon nanotubes and 5–6 nm on the nanospheres.

4.5. *Other precursors*

4.5.1. *Isonitrile precursors **12** and Pt(MeNC)$_2$Me$_2$, **13***

The isonitrile ligands which coordinate the metal as carbenes have been used in the synthesis of precursors for platinum OMCVD. CVD was carried out at 2 × 10^{-3} Torr at 200–250 °C on various substrates (glass, copper, alloys) with a growth rate of 10 nm min^{-1} [67]. The presence of hydrogen in all cases allows the deposition temperature to be as low as 150 °C. At this temperature, the kinetics can be notably accelerated by UV irradiation [34]. Very pure platinum is obtained by this method after a surface stripping step.

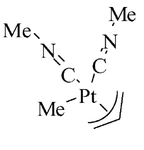

12

Table 2
Analytic results for comparative deposits from Puddephatt et al. [65]

Precursor	H_2 presence	Anal. XPS (at.%)		
		Pt	C	O
$PtMe_2(MeNC)_2$	No	88	11	–
	Yes	95	5	–
(cod)$PtMe_2$	No	86	10	4
	Yes	94	4	2
(cod)CpPtMe	**No**	**77**	**19**	**4**
	Yes	**95**	**5**	**–**
(cod)PtMeCl	**No**	**70**	**25**	**5**
	Yes	**88**	**9**	**3**
CpPtMe (CO)	**No**	**71**	**27**	**2**
$CpPtMe_3$	No	74	25	1
CpPt (η^3-C_3H_5)	**No**	**60**	**38**	**2**
[(acac)$PtMe_3$]$_2$	**No**	**66**	**30**	**4**

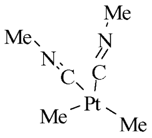

13

4.5.2. *Other cyclopentadienyl ligand containing precursors: (MeCp)Pt(η^3-C_3H_5), **15***

Use of precursor **15** allowed for the deposition of 600 nm thick platinum films at 300 °C on glass with no predominant crystallites orientation [73]. The precursor is vaporized at only 30 °C under reduced pressure and the deposit is carried out with a nitrogen flow (50 sccm) resulting in a total pressure of 20 mbar. Oxygenated and carbonaceous impurities are present on the film surfaces but are almost non-detectable in-depth; a good result in terms of purity.

Other precursors have been reported, often resulting in poorer deposit purity. A series of deposits was carried out by Dryden et al. on various substrates at 250 °C [67]. The new precursors (in bold in Table 2) lead to carbon-rich deposits, especially in absence of hydrogen.

Xue et al. also compared other new precursors with those previously described [52]. The deposits obtained with these new precursors (in bold in Table 3) are not very interesting in terms of deposit purity. Recall that precursors carrying a CO ligand are rather unstable and not easily stored.

Among all the precursors mentioned so far, the use of Pt(acac)$_2$ **1** [41,74], and its asymmetric derivatives [50], of the family of CpPtMe$_3$ **6**, **7** and **8** [59,65], (Me$_2$cod)Pt(Me)$_2$, **17** [75], and (TMEDA)PtMe$_2$ **18** [76] are patented for CVD processes.

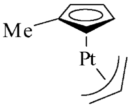

15

Table 3
Summary of previous studies of platinum CVD from Xue et al. [50]

Precursor	Source, θ (°C)	Deposition, θ (°C)	Carrier gas	Impurities (at.%)
$Pt(acac)_2$	150	550	Vacuum	50% C
$Pt(PF_3)_4$	125	400	$H_2 + CO$	5% P
$Pt(CO)_2Cl_2$	25	250	H_2	<1% C, Cl
$CpPtMe_3$	25	180	H_2	<1% C, O
$MeCpPtMe_3$	25	120	H_2	<1% C, O
$PtMe_2(MeCN)_2$	40–120	250	H_2	5% C
$(cod)PtMe_2$	40–120	250	H_2	4% C, 2% O
(cod)(Cp)PtMe	**40–120**	**250**	**H_2**	**5% C**
(cod)PtMeCl	**40–120**	**250**	**H_2**	**9% C, 3% O**
CpPtMe(CO)	**40–120**	**250**	**Vacuum**	**27% C, 2% O**
CpPt(allyl)	40–120	250	Vacuum	38% C, 2% O
$(acac)PtMe_3$	**40–120**	**250**	**Vacuum**	**30% C, 4% O**

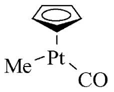

16

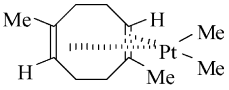

17

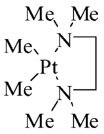

18

5. Carrier or reactive gases?

The nature of the carrier gas was shown in early studies to have a significant effect on the quality of the deposit. Since 1973 [42], Rand showed that post-processing with oxygen at 550 °C eliminated the carbon impurities from the deposit. The effect of this gas was then studied intensively. A two gas mixture for example, hydrogen or oxygen often mixed with an inert carrier gas such as argon, helium or nitrogen provided a particularly notable improvement in the quality of the deposit.

5.1. Hydrogen

The laser CVD studies with $CpPtMe_3$, **6** demonstrated that under the operating conditions used, the deposit obtained in the presence of hydrogen is brilliant with a granular structure, whereas black platinum is obtained with pure argon [10]. A different decomposition mechanism has therefore been proposed where hydrogen intervenes in an oxidative addition on the metal followed by a reductive elimination of cyclopentane and methane (Fig. 6) ligands catalytically hydrogenated off the platinum surface. The surface ligand dissociation is not always complete and it is facilitated by the hydrogen which "cleans" the platinum surface. Use of hydrogen thus permits the preparation of good quality deposits with $MeCpPtMe_3$ **7** [61,77], $Pt(MeNC)_2Me(\eta^3\text{-}C_3H_5)$ **12**, $Pt(MeNC)_2Me_2$ **13** [67], $(cod)Pt(Me)_2$ **14** [27,49,68–71].

Hydrogen due to its reactivity, allows platinum deposition on substrates at lower temperature than under inert gas atmosphere [78]. In the case of **7**, the decomposition is so fast that the film growth rate is, as **6**, limited by the supply of the organometallic species. Nevertheless, the presence of hydrogen is not sufficient to eliminate all carbon impurities [60,62] and can lead, only in certain cases, to better quality films than in the presence of oxygen (*vide infra*) [49].

A moderate concentration of hydrogen (<10%) is necessary to avoid precursor degradation in the vapor phase. In a related research area, the formation of platinum clusters of a minimum size was necessary to initiate the catalytic reaction which results in the hydrogenation of the carbon species [79]. By using $MeCpPtMe_3$ **7**, with a deposition temperature of 175 °C, the deposit's structure is small grained with a high nucleation density and a 6% carbon contain. Under harsher conditions, in the presence of oxygen and with a deposition temperature of 350 °C, the grains are coarser and the film contains 6% carbon and 2% oxygen [39]. With $Pt(acac)_2$, **1**, the decomposition rate is accelerated by hydrogen use, but decomposition itself remains incomplete and the quality of the film is not substantially improved [80]. For certain applications, the use of hydrogen is

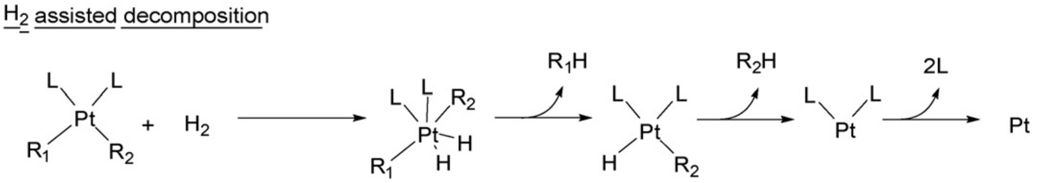

Fig. 6. Hydrogen assisted decomposition mechanism of platinum precursor during deposition.

prohibited because it degrades the platinum film's electric properties (electrical resistivity, residual resistivity ratio, electron mean free paths) [38,40].

5.2. Oxygen

The use of 3% oxygen in the carrier gas leads to deposits with a high degree of crystallinity at 450 °C, when $Pt(acac)_2$, **1** is used [43]. As is the case for hydrogen, oxygen causes a marked reduction of the carbon impurities. When $MeCpPtMe_3$, **7** is used, the deposited film contains surface carbon impurities which can be partially eliminated by sputtering abrasion whereas in the presence of hydrogen, the deposit contains carbon throughout the film [60,62]. Under the conditions described, by carrying out the deposit at 350 °C, nucleation is favoured, producing a film with only few holes. At higher temperature, it is the crystallites' growth which controls the deposit formation and hence the deposit presents significant cavities. When $Pt(hfa)_2$, **2** was used, the use of oxygen also provided a more homogeneous crystallite orientation normal to the surface [48,81].

Oxygen cleaves the ligands more effectively than hydrogen, but also forms a partial oxide layer over peripheral platinum (not detectable by XRD or SEM) which reduces the film surface and grain boundary energies and allows a better film adhesion (damping). The resistivity of the more homogeneous films obtained are not affected because the platinum oxides possibly formed are conductive [48]. Nevertheless, the use of $Pt(acac)_2$, **1** gives poorer results than $MeCpPtMe_3$, **7** in terms of grains size (>25 nm for $Pt(acac)_2$, **1** and >50 nm for $MeCpPtMe_3$, **7**) and orientation, but better results in term of purity and substrate coverage ratio [38,44]. In this example, the precursor $Pt(acac)_2$, **1** appears to be competitive with $MeCpPtMe_3$, **7**.

The effect of oxygen was studied much more closely with $MeCpPtMe_3$, **7** than with $CpPtMe_3$, **6** [82–84]. Similarly to hydrogen, oxygen permits a drastic reduction in the deposition temperature and a decrease in the duration of the initiation step. Oxidative decomposition of the complex is catalysed by the oxygen adsorbed on the platinum surface. All the adsorbed oxygen is consumed and the effect of the oxygen pressure is limited by the matter transfers. The growth rate of the film is thus linear over time due to the surface saturation of adsorbed oxygen. The surface energy is thus decreased and at high temperature (300 °C) grain formation takes place. However, too high a flow of oxygen can be detrimental to the film quality: at too high a concentration, it provokes structural defects and the film growth is less regular. With $EtCpPtMe_3$, **8**, oxygen action allows a quick platinum film formation which catalyses further precursor decomposition. At very high concentration ($O_2/Ar = 7:1$), inhibition of precursor adsorption onto the film occurs and a decrease in growth is observed. Generally, the presence of oxygen results in high quality films (conductivity, structure, etc.) [40]. In the case of the ALD process, the use of oxygen is absolutely necessary.

5.3. Other used gases for Pt CVD

Water vapor accelerates the decomposition of the precursor $MeCpPtMe_3$, **7** on glass [32] and of $Pt(hfac)_2$, **2** on TiN or SiO_2/Si [85]. Indeed, the induction period is shorter if the carrier gas is wet. Additional hydroxyl groups (OH) are probably formed on the substrate surface which initiate the deposit. When sufficiently large platinum clusters are formed, the film growth reaction is catalytically activated. With $Pt(acac)_2$, **1** water causes small grain size (30 nm on quartz) and increases the concentration of nucleation sites [80]. Like hydrogen, water also accelerates the precursor decomposition. Water can replace advantageously oxygen in platinum films deposition. Conceding a drop of the deposition rate toward use of oxygen, water leads to homogeneous randomly oriented grain depositions and low resistivity films. Battiston et al. have demonstrated that resistivity is tightly linked to crystallite size [86], and the bigger the crystallites are, the lower the resistivity is. This trend is valuable only in the case of homogeneous films without preferred orientation and with few voids. With oxygen, above a temperature threshold, enhanced adatoms mobility increases the crystallite dimension and produces ordered grains with voids between them. Moreover, films use to show a non-homogeneous morphology along the position in the reactor in this case. With water, adsorbed water limits platinum atoms diffusion and increasing temperature only makes the grains size bigger keeping them randomly oriented.

The use of a 1:1 mixture $N_2O + O_2$ has also been considered [87,88] and with $MeCpPtMe_3$, **7**, under mild conditions (400 °C, 30 Torr in 120 s), a 96 nm thick film on borophosphosilicate glass can be produced. The reactive oxidant gas can be injected into the medium simultaneously with the precursor and a reducing gas (H_2, NH_3) or sequentially with a fine flow controller that determines the precursor deposition rate [89].

6. The substrates

The chemical nature of the substrates on which the deposits are performed depends obviously on the application concerned. The preparation of solid catalysts often requires the use of oxides (mainly alumina or silica) or nanocarbon particles. One of the required objectives is obtaining a deposit having a high surface area.

Microelectronics uses SiO_2-type oxides, deposited or thermally formed, as well as conducting materials (metals, doped oxides such as SnO_2, diffusion barriers such as TaN) or Si semiconductors. Film homogeneity and excellent conduction properties are required for this type of application.

The chemical nature of the substrate influences the quality of the deposit to a great extent at the early stage of its growth during nucleation. It influences the properties of film adhesion and even the formation of the deposit itself. For example, $MeCpPtMe_3$, **7** forms more adherent films on a SiO_2/Si support when a preliminary TiO_2 oxide film is deposited on the surface. Fig. 7 shows how silanol moieties can help to form early nucleation site on SiO_2 substrates. The films obtained are more homogeneous and smoother however, they also contain more impurities. The Pt crystallites formed on TiO_2 do not demonstrate a preferred orientation and thus have increased surface energy. It is postulated that a growth of crystallites toward a preferred crystallographic orientation leads

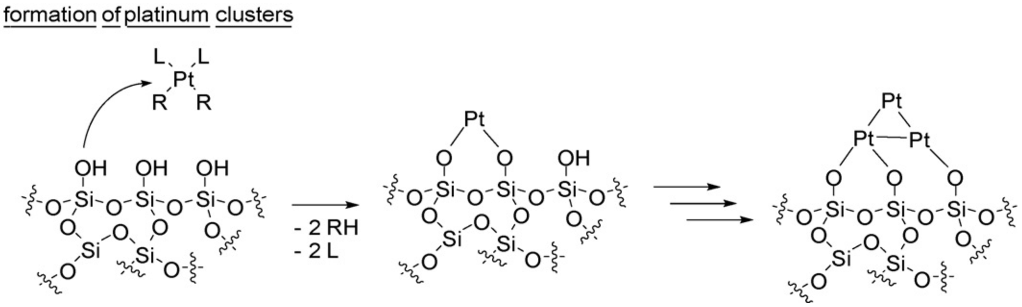

Fig. 7. Formation of platinum clusters by CVD onto SiO_2 leading to nucleation.

to a compact atomic stacking with a weaker surface energy [37].

As previously stated, nucleation is supported by the presence of hydroxyl groups (OH) on the surface. The –OH group density can be increased by the use of steam, but depends also on the chemical nature of the surface. The effect of the hydroxyl group was demonstrated with precursor **1**. The deposition of $Pt(acac)_2$, **1** on CaF_2 at 420 °C at 1 Torr led to a film having a rather rough surface (roughness: 10 nm) and a grain size of 148 ± 8 nm. On quartz, roughness is less significant (4 nm) and the grains are smaller: 123 ± 9 nm. In the presence of steam, the grains are even smaller [39]. Clearly shown here, is the positive correlation between –OH density and increased nucleation (Fig. 7). Moreover, surface pre-treatment with Me_3SiCl counteracted the positive effect of the surface –OH groups due to their masking as trimethyl silyl ethers [90]. The growth on certain surfaces such as metal surfaces or metal oxides is very fast whereas on other surfaces slow growth is observed, hence the deposit can be grown selectively on supports presenting chemically different areas on the surface (some metal nitrides or oxides can be used as catalytically inactive insulation promoting platinum deposition elsewhere, on active regions) [91].

The first tests on graphite (HOPG) highlighted the chemical inertia of the surface with respect to nucleation and the difficulty of depositing platinum onto it [92]. Whereas on SiO_2, there is formation of a deposit at temperatures as low as 140 °C using the precursor $MeCpPtMe_3$, **7**, on graphite, deposition does not occur until 190 °C without an induction period. A decomposition reaction in the gas phase can contribute, in this case, to the nucleation process. A STM (scanning tunnelling microscopy) study revealed non-homogeneous deposits with various structures: clusters of 8–80 Å with some very much larger Pt islands. With $Pt(Me)_2(cod)$, **14**, a polycrystalline deposit is observed on HOPG [36]. Platinum islands of 20–30 nm height which followed the substrate cleavage lines indicated that nucleation occurred mainly along the planes. Few spots are present between the cleavage plans. By increasing the deposition time, one increases the surface coverage rate and dendritic structures appear, connecting the cleavage lines to the nucleation sites on plane surface defects. The oxygenated functional groups are only on the plane section and it is these that allow the nucleation growth. By oxidizing graphite at 650 °C, one increases the number of sites and the platinum film becomes more uniform. The method most usually encountered to increase the number of nucleation sites is to treat the graphite with boiling nitric acid. When depositing the precursor $Pt(Me)_2(cod)$, **14** on carbon fibres, the resulting platinum content is more homogeneous and the crystallite size is larger (4–5 nm) on the support. Fig. 8 shows an example of such dispersion.

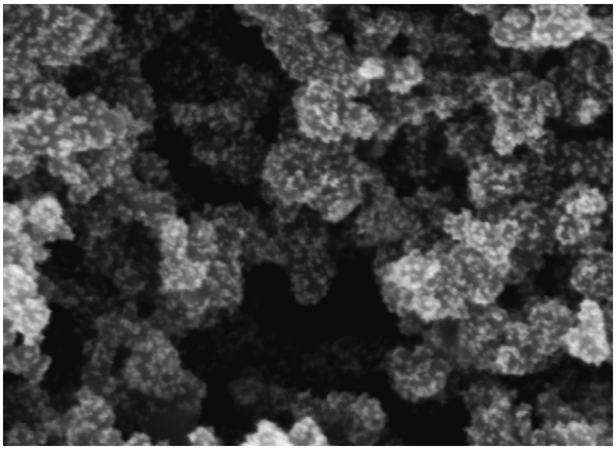

Fig. 8. SEM picture of a particle dispersion of platinum on a graphite support. Size of the grains reaches 5–10 nm.

As the surface of graphite is particularly inert, the role of the nitric acid is to partially oxidize this surface and to form carboxylic acid groups (–COOH). Anchoring can then be done through carboxylate–platinum connections. Hence, the cluster $Pt_4(CH_3COO)_8$ is a known example of an isolable compound containing this type of bond. This method of support activation was also employed with nanospheres and carbon nanotubes [71,72] for which standard thermal platinum OMCVD is impossible.

7. Nucleation and growth

According to the operating conditions used, the precursor flow can be the main contributor to the nucleation process, i.e. by the formation of new crystallites or with the growth of the initially formed crystallites. Under conditions favouring nucleation, the film obtained appears as a small crystallites, the consequent aggregation of which results in good connectivity between the grains and nearly an absence of holes and hence, a low resistivity. Under conditions supporting growth, the film is made up of large crystallites. Various physical factors influence the prevalence of nucleation or growth at the time of film formation. Due to this parameter being of a kinetic nature, the temperature is very important, the phenomena of growth and nucleation not utilizing same activation energies.

Kwon and Yoon highlighted that in the case of the deposition carried out with $MeCpPtMe_3$, **7**, the film morphology was controlled by nucleation at 350 °C and by the growth at 450 °C. With $EtCpPtMe_3$, **8**, at high temperatures (>400 °C) deposition is controlled by the mass transfer and film growth is predominant. In this case, the film obtained contains many holes which increase its resistivity and its quality is improved by lowering the pressure [60]. Increasing the temperature favours the growth of crystallites, leads to a smoother surface and to a higher deposition rate, but to poor support coverage; while low temperature leads to a higher concentration of impurities (mainly carbon), because of partial precursor decomposition. Traditionally, oxygen is added during the deposition process to suppress this phenomenon. Likewise, Goswami et al. showed that under mild conditions (in the presence of hydrogen at 175 °C) small grains (high nucleation) were obtained containing 6% of carbon, whereas under harsher conditions (in presence of oxygen at 350 °C) coarse grains were obtained containing 6% of carbon and 2% of oxygen [39]. The authors do not comment on the effect that the gas composition has on the nucleation but we can link this phenomenon to what is observed with adsorbed water: limitation of atom diffusion and then of crystal growth. Nucleation can be supported by the nature of the substrate at the beginning of deposition and also by the nature of the gas used. For example, the addition of steam that will produce hydroxy groups; the consequences of which are described above. Nucleation is also supported by precursor "supersaturation" (*vide infra*), obtained by increasing the precursor concentration in the phase gas. Decomposition in phase gas can also contribute to the nucleation process [92].

Generally during deposition, small grains are formed by nucleation on the substrate surface initially; bigger grains are then formed onto this first layer. A process has been developed in order to produce smooth films with small grains throughout the thickness of the film [93], and for that purpose, the deposit is performed in two stages. First, the growth conditions support nucleation, the agglomeration and the formation of a smooth initial film. Second, film growth with small grains is favoured. When the quantity of evaporated precursor for the formation of the initial film is reached, the operating conditions are changed; the temperature, the pressure and the oxidizing concentration being lowered.

8. Autocatalysis

In the case of deposits under "normal" conditions, in absence of reactive carrier gases such as oxygen or hydrogen, an induction period is often observed where the film formation kinetics are slow. After this period, the kinetics are strongly accelerated. The period of induction is considerably shorter if the gas is wet or contains hydrogen.

This phenomenon of autocatalysis was highlighted in the early stages of platinum OMCVD experiments. Hence, beyond an induction period, one observes that the deposition already formed catalyses the decomposition of the precursor and accelerates further film formation. The method of formation and the crystalline nature of this layer are important. A non-crystalline platinum layer may be unable to catalyse further platinum CVD deposition. In the case of a silica substrate supporting a discontinuous layer of non-crystalline platinum formed by vacuum evaporation, CVD platinum settles only on the zone where this first layer was absent [94]. Furthermore, platinum crystallites formed by CVD on SiO_2 grow faster than on non-crystalline platinum deposited by vacuum evaporation. Five-micrometer crystallites of platinum are obtained and their adhesion, in this case, is poor. The growth initiation stage corresponds to the formation of platinum clusters which allow the catalytic formation of the deposit [95]. This stage is determined by the nucleation process. The energy necessary for the growth of the deposit on platinum is less than on a virgin support (Si/SiO_2, etc.). At low oxygen pressure and low temperature, the film growth rate becomes fast when one deposits on a pre-formed platinum layer [82]. Platinum particles can also catalyse the decomposition of organometallic precursors other than platinum precursors. Small platinum particles, obtained by deposition of $(cod)Pt(Me)_2$, **14** in a mixture of helium with 3% hydrogen at 120 °C, thus allows the deposition of palladium at a temperature as low as 60 °C with $(hfac)Pd(\eta^3\text{-}C_3H_5)$ [67]. The catalytic effect here is clearly highlighted. Conversely, the platinum deposition on polystyrene beads is possible between 70 and 85 °C with $(cod)Pt(Me)_2$, **14** in the presence of a catalytic quantity of $(hfac)Pd(C_4H_7)$ [96]. Palladium grains are deposited at low temperature and initiate the platinum deposition.

9. Mass transfer and supersaturation

In conventional CVD, high concentrations of precursor in the gas phase are maintained by a high precursor partial pressure. This improves the nucleation rate and increases the homogeneity and density of the film, which is composed of fine particles [49]. The phenomenon of "supersaturation" can be achieved by heating the precursor while placing the substrate in a turbulent gas flow which supports the mass transfer. This approach is used in the fluidized bed deposition process. Hence, deposition in fluidized bed studies of carbon nanospheres and graphite stems showed that increasing the precursor partial pressure by 25 times (at higher sublimation temperature) resulted in 15 times smaller particles, dispersed in a homogeneous fashion [27].

10. Precursor decomposition

Decomposition of the precursor is a key stage in the formation of the film. Fast and complete precursor decomposition usually ensures that a film of good purity and a good quality is obtained. The chemical nature of the precursor is the dominant factor here, requiring stability under the vaporization conditions and decomposition only under the deposition conditions. Compared to other metals, the catalytic properties of platinum are especially suited to this process.

In the presence of hydrogen, platinum behaves as a hydrogenation catalyst. There is precursor adsorption on the surface, then oxidative addition of hydrogen and reductive elimination of a hydrocarbon. Thus, $CpPtMe_3$, **6** liberates methane and cyclopentane and $(cod)Pt(Me)_2$, **14** affords methane and cyclooctane. The formation of platinum-hydride species was highlighted by the isomerization of C=C double bonds [33]. The use of oxygen results in water and carbon dioxide production.

In the absence of reactive gases, the proposed mechanisms differ according to the nature of the precursor. The formation of coupling products is observed, thus the complex $Pt(MeNC)_2Me(\eta^3\text{-}C_3H_5)$, **12** produces ethane and 1,5-hexadiene by intermolecular coupling [67]. In this case, two pathways are proposed: reaction on the platinum surface or a radical mechanism. With $Pt(\eta^3\text{-}C_3H_5)_2$ **9**, the proposed decomposition mechanism occurs by α-elimination which affords a vinylidene. Propene can depart or vinyl C–H activation occurs, leading to a metallacyclobutene. Cycloreversion of the latter species leads to a metal methylene moiety with acetylene release; β-elimination leading to an allene is also discussed [66].

Certain precursors can lead to films selectively deposited onto certain surfaces by a transmetallation redox mechanism. Hence, $Pt(hfa)_2$, **2** will deposit platinum at low temperature on copper and iron, but not on silicon. A TPRS (temperature-programmed reaction spectroscopy) study showed that deposition was accomplished according to the following steps [97]:

- at 100 K: adsorption of the precursor.
- at 175 K: loss of a hfa (and hfa-Cu formation).
- at 283 K: loss of the second hfa, release of $Cu(hfa)_2$.
- at 450 K: partial decomposition of adsorbed hfa; Pt, CO, CF_3 remain adsorbed.
- at 800 K: Pt, C remain adsorbed.

A limit to the transmetallation process is the formation of a Pt layer on copper at low temperature. At higher temperature, there is copper diffusion to form a Pt–Cu alloy that makes this reaction possible.

11. Conclusions

General methods of platinum OMCVD have been summarized in this article. Two different objectives have been investigated throughout these studies: some methods aim at the enhancement of deposit purity, rate and yield. Other methods aim at the formation of local deposits, especially to form 3D objects: lines, spots, etc. LCVD and EBCVD are good examples of the latter allowing the formation of sub-micro-objects using these techniques. Very good results can be obtained due to the availability and versatility of precursors having good volatility and a good thermal stability window. The best systems are $MeCpPtMe_3$, **7** and $EtCpPtMe_3$, **8** this one being oxygen and water stable at ambient temperature. On the other hand, $(cod)Pt(Me)_2$, **14** is less volatile but it is easily synthesized in high yield and also gives very interesting results. These precursors benefit from facile decomposition under the CVD conditions. Decomposition is particularly effective and rapid in the presence of oxidizing or reducing gases. The contribution of hydrogen and oxygen as reactive gases also allows notable improvements in the quality of the film deposited and experimental conditions (lowering temperature in particular). Films have therefore been obtained with only traces of impurities, carbon being the most common. A good understanding of nucleation and growth mechanisms has enabled fine-tuning of operating conditions to improve the rate of deposition and purity, while also allowing formation of local deposits according to the surface chemistry. OMCVD remains a dynamic process with many complex factors that are not always taken in account: e.g. reactor geometry.

An update of the intervening mechanisms in the deposition process should also allow further development and better control, according to the parameters such as the nature of the support and the gas.

Acknowledgements

This work is partially supported by the French Agence Nationale pour la Recherche in the PAN-H program framework under the project INNOVAME, contract ANR-05-PANH-016. We acknowledge Dr. Alexander Yuen for the English reviewing of the paper.

References

[1] D.C. Bradley, Polyhedron 13 (1994) 1111.

[2] M.J. Hampden-Smith, T.T. Kodas, Chem. Vap. Depos. 1 (1995) 8.

[3] J.R. Vargas Garcia, T. Goto, Mater. Trans. JIM 44 (2003) 171.

[4] D.M. Dobkin, M.K. Zuraw, Principles of Chemical Vapor Deposition, Kluwer Academic Publishers, Dordrecht, 2003.

[5] D. Braichotte, C. Garrido, H. van den Bergh, Appl. Surf. Sci. 46 (1990) 9.

[6] C. Garrido-Suarez, D. Braichotte, H. van den Bergh, Appl. Phys. A 46 (1988) 285.

[7] D. Braichotte, H. van den Bergh, Appl. Phys. A 44 (1987) 353.

[8] H.H. Gilgen, T. Cacouris, P.S. Shaw, R.R. Krchnavek, R.M. Osgood, Appl. Phys. B 42 (1987) 55.

[9] C. Garrido, H. van den Bergh, J. Appl. Phys. 70 (1991) 966.

[10] L. Koplitz, D.K. Shuh, Y.-J. Chen, R.S. Williams, J.I. Zink, Appl. Phys. Lett. 53 (1988) 1705.

[11] E.P. Marsh, US Patent US 6204178 B1 (2001).

[12] E.P. Marsh, US Patent Appl. 2006/0014367 A1 (2006).

[13] E. Feurer, S. Kraus, H. Suhr, J. Vac. Sci. Technol. A 7 (1989) 2799.

[14] A.D. LaLonde, M.G. Norton, D.N. McIlroy, D. Zhang, R. Padmanabhan, A. Alkhateeb, H. Han, N. Lane, Z. Holman, J. Mater. Res. (2005) 549.

[15] J. Pulpytel, C. Petit Etienne, F. Arefi-Khonzari, Trans. Plasma Sci. 33 (2005) 244.

[16] M. Kadowaki, H. Yoshizawa, M.M. Suzuki, Thin Solid Films 506–507 (2006) 123.

[17] K.A. Telari, B.R. Rogers, H. Fang, L. Shen, R.A. Weller, D.N. Braski, J. Vac. Sci. Technol. B 20 (2002) 590.

[18] T. Tao, J. Ro, J. Melngailis, Z. Xue, H.D. Kaesz, J. Vac. Sci. Technol. B 8 (1990) 1826.

[19] J. Melngailis, P.G. Blauner, Mater. Res. Soc. Symp. Proc. 147 (1989) 127.

[20] U. Hübner, R. Plontke, M. Blume, A. Reinhardt, H.W.P. Koops, Microelectr. Eng. 57–58 (2001) 953.

[21] M. Takai, T. Kishimoto, H. Morimoto, Y.K. Park, S. Lipp, C. Lehrer, L. Frey, H. Ryssel, A. Hosono, S. Kawabuchi, Microelectr. Eng. 41/42 (1998) 453.

[22] H.W. Koops, A. Kaya, M. Weber, J. Vac. Sci. Technol. B 13 (1995) 2400.

[23] D. Beaulieu, Y. Ding, Z.L. Wang, W.J. Lackey, J. Vac. Sci. Technol. B 23 (2001) 2151.

[24] A. Botman, J.J.L. Mulders, R. Weemaes, S. Mentink, Nanotechnology 17 (2006) 3779.

[25] B.W. Kempshall, L.A. Giannuzzi, B.I. Prenitzer, F.A. Stevie, S.X. Da, J. Vac. Sci. Technol. B 20 (2002) 286.
[26] S. Wang, Y.-M. Sun, Q. Wang, J.M. White, J. Vac. Sci. Technol. B: Microelectr. Nanometer Struct. 22 (4) (2004) 1803.
[27] C. Vahlas, F. Juarez, R. Feurer, P. Serp, B. Caussat, Chem. Vap. Depos. 8 (2002) 127.
[28] T. Aaltonen, M. Ritala, T. Sajavaara, J. Keinonen, M. Leskelä, Chem. Mater. 15 (2003) 1924.
[29] T. Aaltonen, A. Rahtu, M. Ritala, M. Leskelä, Electrochem. Solid-State Lett. 6 (2003) C130.
[30] M. Utriainen, M. Kröger-Laukkanen, L.-S. Johansson, L. Niinistö, Appl. Surf. Sci. 157 (2000) 151.
[31] P. O'Brien, N.L. Pickett, D.J. Otway, Chem. Vap. Depos. 8 (2002) 237, and internal references.
[32] P.K. Baumann, P. Doppelt, K. Fröhlich, L. Gueroudji, V. Cambel, D. Machajdik, M. Schumacher, J. Lindner, F. Schienle, D. Burgess, G. Strauch, H. Juergensen, H. Guillon, C. Jimenez, Integr. Ferroelectrics 44 (2002) 135.
[33] C.D. Tagge, R.D. Simpson, R.G. Bergman, M.J. Hostetler, G.S. Girolami, R.G. Nuzzo, J. Am. Chem. Soc. 118 (1996) 2634.
[34] B. Nixon, P.R. Norton, E.C. Ou, R.J. Puddephatt, S. Roy, P.A. Young, Chem. Mater. 3 (1991) 222.
[35] M. Labeau, B. Gautheron, F. Cellier, M. Vallet-Regi, E. Garcia, J.M. Gonzàlez Calbet, J. Solid State Chem. 104 (1993) 434.
[36] M. Aktary, C.E. Lee, Y. Xing, S.H. Bergens, M.T. Dermott, Langmuir 16 (2000) 5837.
[37] O. Valet, P. Doppelt, P.K. Baumann, M. Schumacher, E. Balnois, F. Bonnet, H. Guillon, Microelectron. Eng. 64 (2002) 457.
[38] J. Goswami, C.-G. Wang, S.K. Dey, Chem. Vap. Depos. 9 (2003) 213.
[39] J. Goswami, P. Majhi, C.G. Wang, S.K. Dey, Integr. Ferroelectrics 42 (2002) 13.
[40] H.-J. Sun, E.S. Choi, S.Y. Kweon, N.K. Kim, S.J. Yeom, J.-S. Roh, H.-C. Sohn, J.W. Kim, Jpn. J. Appl. Phys. 43 (5A) (2004) L624.
[41] E.C. Marboe, US Patent US2430520 (1947).
[42] M.J. Rand, J. Electrochem. Soc. 120 (1973) 686.
[43] B.S. Kwak, P.N. First, A. Erbil, B.J. Wilkens, J.D. Budai, M.F. Chisholm, L.A. Boatner, J. Appl. Phys. 72 (1992) 3735.
[44] G. Malandrino, R. Lo Nigro, I.L. Fragalà, Chem. Vap. Depos. (1999) 59.
[45] L. Helm, L.I. Elding, A.E. Marbach, Inorg. Chem. 24 (1985) 1719.
[46] C.T. Mortimer, Rev. Inorg. Chem. 6 (1984) 233.
[47] T.P. Martin, C.P. Tripp, W.J. DeSisto, Chem. Vap. Depos. 11 (2005) 170.
[48] J.M. Lee, C.S. Hwang, H.-J. Cho, C.-G. Suk, H.J. Kim, J. Electrochem. Soc. 145 (1998) 1066.
[49] J.-C. Hierso, R. Feurer, P. Kalck, Chem. Mater. 12 (2000) 390.
[50] Y. Atsuya, T. Nobuki, Jpn. Kokai Tokkyo Koho, JP 2004203744 (2004).
[51] M.J. Rand, J. Electrochem. Soc. 122 (1975) 811.
[52] Z. Xue, H. Thridandam, H.D. Kaesz, R.F. Hicks, Chem. Mater. 4 (1992) 162.
[53] T. Kruck, K. Baur, Zeit. Annorg. Allg. Chem. 364 (1969) 192.
[54] J.C. Marriott, J.A. Salthouse, M.J. Ware, J.M. Freeman, J. Chem. Soc. D: Chem. Commun. (1970) 595.
[55] J.M. Morabito, M.J. Rand, Thin Solid Films 22 (1974) 293.
[56] J.E. Gozum, D.M. Pollina, J.A. Jensen, G.S. Girolami, J. Am. Chem. Soc. 110 (1988) 2688.
[57] Y.-J. Chen, H.D. Kaesz, H. Thridandam, R.F. Hicks, Appl. Phys. Lett. 53 (1988) 1591.
[58] L.D. Boardman, R.A. Newmark, Magn. Reson. Chem. 30 (1992) 481.
[59] S.H. Meiere, C.A. Hoover, WO 03/106011 A2 (2003).
[60] J.-H. Kwon, S.-G. Yoon, Thin Solid Films 303 (1997) 136.
[61] Z. Xue, M.J. Strouse, D.K. Shuh, C.B. Knobler, H.D. Kaesz, R.F. Hicks, R.S. Williams, J. Am. Chem. Soc. 111 (1989) 8779.
[62] J.-H. Kwon, S.-G. Yoon, J. Electrochem. Soc. 144 (1997) 2848.
[63] W.-G. Choi, E.-S. Choi, S.-G. Yoon, Chem. Vap. Depos. 9 (2003) 321.
[64] N. Hiroshi, M. Hideaki, S. Norio, Jpn. Kokai Tokkyo Koho, JP 2005029851 (2005).
[65] H. Kadokura, US Patent 5,929,267 (1999).
[66] R.U. Kirss, Appl. Organomet. Chem. 6 (1992) 609.
[67] N.H. Dryden, R. Kumar, E. Ou, M. Rashidi, S. Roy, P.R. Norton, R.J. Puddephatt, Chem. Mater. 3 (1991) 677.
[68] J.-C. Hierso, R. Feurer, J. Poujardieu, Y. Kihn, P. Kalck, J. Mol. Catal. A 135 (1998) 321.
[69] J.-C. Hierso, P. Serp, R. Feurer, P. Kalck, Appl. Organomet. Chem. 12 (1998) 161.
[70] P. Serp, J.-C. Hierso, R. Feurer, Y. Kihn, P. Kalck, J.-L. Faria, A.E. Aksoylu, A.M.T. Pacheco, J.L. Figueiredo, Carbon 37 (1999) 527.
[71] P. Serp, J. Feurer, Y. Kihn, P. Kalck, J.L. Faria, J.L. Figueiredo, J. Mater. Chem. 11 (2001) 1980.
[72] P. Serp, R. Feurer, Y. Kihn, P. Kalck, J.L. Faria, J.L. Figueiredo, J. Phys. IV (2002) Pr4/29.
[73] G. Rossetto, P. Zanella, G. Carta, R. Bertani, D. Favretto, G.M. Ingo, Appl. Organomet. Chem. 13 (1999) 509.
[74] J.F. Ackerman, P.V. Arszman, Eur. Pat. EP 1518942 (2005).
[75] S. Atsushi, U. Hiroto, S. Masamitsu, O. Katsumi, Jpn. Kokai Tokkyo Koho JP8157490 (1996).
[76] U. Hiroto, S. Atsushi, S. Masamitsu, O. Katsumi, Jpn. Kokai Tokkyo Koho JP 8176177 (1996).
[77] H.D. Kaesz, R.S. Williams, R.F. Hicks, Y.-J.A. Chen, Z. Xue, D. Xu, D.K. Shuh, H. Thridandam, Mater. Res. Symp. Proc. 131 (1989) 395.
[78] R. Kumar, S. Roy, M. Rashidi, R.J. Puddephatt, Polyhedron 8 (1989) 551.
[79] A. Zinn, B. Niemer, H.D. Kaesz, Adv. Mater. 4 (1992) 375.
[80] S. Barison, M. Fabrizio, G. Carta, G. Rossetto, P. Zanella, D. Barreca, E. Tondello, Thin Solid Films 405 (2002) 81.
[81] J.M. Lee, S.-K. Hong, C.S. Hwang, H.J. Kim, J. Korean Phys. Soc. 33 (1998) S148.
[82] M. Hiratani, T. Nabatame, Y. Matsui, K. Imagawa, S. Kimura, J. Electrochem. Soc. 148 (2001) C524.
[83] M. Hiratani, T. Nabatame, Y. Matsui, S. Kimura, Electrochem. Solid-State Lett. 5 (2002) C28.
[84] M. Hiratani, T. Nabatame, Y. Matsui, S. Kimura, Thin Solid Films 410 (2002) 200.
[85] N.L. Jeon, W. Lin, M.K. Erhardt, G.S. Girolami, R.G. Nuzzo, Langmuir 13 (1997) 3833.
[86] G.A. Battiston, R. Gerbasi, A. Rodriguez, Chem. Vap. Depos. 11 (2005) 130.
[87] G.J. Dederian, US Patent Appl. US 2002/0000591 A1 (2002).
[88] G.J. Derderian, US Patent US 6750110 B1 (2004).
[89] W. Li, S. Yang, US Patent Appl. US 2003/0049932 A1 (2003).
[90] J.O. Williams, Adv. Mater. 1 (1989) 282.
[91] W. Hartner, F. Hintermaier, G. Schindler, US Patent Appl. US 2002/0090450 A1 (2002).
[92] T. Ngo, L. Brandt, R.S. Williams, H.D. Kaesz, Surf. Sci. 291 (1993) 411.
[93] G.J. Derderian, G.S. Sandhu, US Patent Appl. US 2002/0048940 A1 (2002).
[94] B. Lecohier, J.-M. Philipoz, H. van den Bergh, J. Vac. Sci. Technol. B 10 (1992) 262.
[95] R.J. Puddephatt, Polyhedron 13 (1994) 1233.
[96] M. Feng, R. Puddephatt, J. Chem. Mater. 15 (2003) 2696.
[97] E.L. Crane, Y. You, R.G. Nuzzo, G.S. Girolami, J. Am. Chem. Soc. 122 (2000) 3422.